Arrested Melting due to Strain in Ultrahigh Molecular Weight Polyethylene

H. Phuong-Nguyen and G. Delmas*

Chemistry Department, Université du Québec à Montréal, CP 8888 Suc A, Montreal, H3C 3P8 Canada

Received December 26, 1989; Revised Manuscript Received September 11, 1991

ABSTRACT: Using the sensitive and stable Setaram microcalorimeter C80, the melting and crystallization traces of ultrahigh molecular weight polyethylene GUR have been obtained at low rates of heating/cooling (v = 0.5, 1, 3, 6, 12 K/h). Slow heating permits identification of three fractions associated respectively with the melting of low molecular weights (I), unconstrained crystals (II), and constrained crystals (III). Melting is arrested between fractions II and III during a time/temperature gap which depends on the thermal history of the sample. Fraction III is found to be highly superheatable, not being able to melt completely below 200 °C if v is higher than 12 K/h. Including H_3, the heat of fusion of fraction III, the overall crystallinity is found to be high, respectively 0.87 and 0.94 for the as-received and annealed samples. The equilibrium melting temperatures are about 137 for T(I), 141 for T(II), and above 155 °C for T(III). The high crystallization temperature of fraction III (>155 °C) reveals that strain in the melt is stable in time/temperature above melting. Heat flows at fusion and crystallization suggest that a hexagonal phase forms between solid and melt in fraction III. The increase of fraction III after slow crystallization links perfection of crystals and strained melting. The possibility that the high-temperature endotherm has another origin than the melting of strained crystals is discussed.

Introduction

The present research was initiated to understand better the process of dissolution of ultrahigh molecular weight polyethylene (UHMWPE) in a solvent and recrystallization as a gel. The homogeneity of the solution and of the subsequent gel seems not to have attracted much attention. In order to facilitate dissolution and since the process was feasible with the Setaram C80 calorimeter, dissolution was achieved at a slow rate of heating. Although the main features of the slow melting can be found in the slow dissolution,[1] we report first the change of phase with only one component which is simpler to present.

Another reason to study slow melting or dissolution derives from the mention in the literature of slow and incomplete melting[2,3] in the case of extended-chain crystals and shish kebabs. Partial melting could explain the discrepancy reported for UHMWPE between the low value of crystallinity measured by calorimetry (0.7)[4,5] and the higher ones obtained by other methods (density,[6,7] proton mobility,[8] IR, and X-ray analyses[7]) which do not entail melting. The lack of homogeneity of the melt is also suggested by T2 relaxation results. A fast and a slow relaxation have been observed, and their respective weights depend on the thermal history of the melt.[9]

Pressure raises the free energy of crystals and of liquids, but the effect is larger on the melt (v(amorphous) > v(crystal)) so that the melting temperature T_m of crystals is increased by pressure. Strain on crystals changes T_m in the same direction as P does, but it has another effect, namely, to slow the melting if extended-chain crystals are formed. Strain can be imposed externally on a fiber for instance by tightening its extremities or chemically by forming cross-links between the chains. Strain which can also be built into the sample during polymerization[4,5,10,11] increases with the perfection of the crystals but also with the concentration of long chains and of tie molecules. A quantitative correlation between strain and the increase of T_m will be discussed below.

When solid polyethylene (PE) is heated, while under pressure or under strain, it goes through an intermediate disordered crystalline phase (the pseudohexagonal phase) before complete melting.[12,13] This phase has been identified by X-ray diffraction or by differential scanning calorimetry (DSC). During melting of strained fibers, the two distinct endotherms found within a few Kelvin of each other have been associated respectively with the orthorhombic–hexagonal transition and the hexagonal–melt transition.[14,15] When the sample submitted to melting is constituted of homogeneous and perfect crystals grown under pressure (with a high molecular weight (MW)), there is a moderate but not negligible rise of melting temperature due to the strain induced by the connections between crystals.

In order to obtain $T_{m,o}$, the equilibrium melting temperature of such extended-chain crystals, the connections between crystals are severed by etching,[16] leading to $T_{m,o}$ = 141 °C, a value 5 K lower than that obtained previously.[17] Since strain and tie molecules have been advanced to explain the reflections found below and above melting of UHMWPE,[4,11] its thermal properties,[4] and the birefringence at high temperature in the PE melt,[17] it seemed that, apart from the understanding of gel formation, there was some interest in investigating the strain in nascent UHMWPE by submitting it to slow melting.

Equilibrium melting temperatures can be approached by a step by step heating,[18] and the progress of melting can be followed by birefringence or specific volume.[19] An alternative method is to use a very slow temperature ramp in a calorimeter to detect the on-going fusion by the heat flow. During the slow melting, reorganization will occur in the solid,[3] defects will move and concentrate in disordered regions situated in between blocks of more ordered crystals, lamellar crystals will be thickened, and overall crystallinity will increase. The perfection of crystals is likely to slow the kinetics of melting in the high-temperature range. Fractionation by molecular weight noted at higher rate will be more extensive.

In the present work, traces of fusion and crystallization of UHMWPE at slow rates of heating are presented. Some results are given also on medium MW PE.

0024-9297/92/2225-0408$03.00/0

Experimental Section

Polymer. The ultrahigh molecular weight (UHMW) sample is a Hostalen GUR 413 (Hoechst) whose nominal molecular weight is 0.9×10^6. The nascent samples were used as such or annealed in different conditions under a nitrogen atmosphere. Melting traces are obtained after a residence of 1 week either at 120 °C in the dry state or at 90 °C with a solvent. The solvent was evaporated at the same temperature and the sample dried completely under vacuum at room temperature. The medium and low molecular weight samples whose melting traces have been obtained are the following: NIST 1483 (US), M_w = 32 100, M_w/M_n = 1.11; NIST (US), M_w = 119 600, M_w/M_n = 1.19; and Marlex (Philips), M_w = 155 000, M_w/M_n = 10.

Calorimeter. The Setaram C80 calorimeter is a sensitive differential calorimeter equipped with large cells suitable for solution work. The sample (10–40 mg) and 2 mL of mercury for good thermal contact are placed in a glass tube which is sealed after bubbling nitrogen for 2 h. The Setaram calibrations for temperature and heat were checked with the melting trace of indium.

With a slow heating rate (v = 0.5, 1 K/h), the background noise is about 5 μV after smoothing of the spikes in the signal. Since the software of one of the calorimeters was not equipped with this smoothing device, no correction was made on the curves. The change of the baseline at high temperature is due to the expansion of mercury which is not exactly the same on both sides. The endotherm situated after the main peak (fractions I + II) has been called fraction III. It stands out better when a blank signal is subtracted from the melting trace. However, preparing an exact blank by adjusting exactly the weight of the sealed glass tube and of the mercury could not be performed for each sample. It was useful though to confirm the analysis of the high-temperature endotherms. Recent results using a device where substraction can be done routinely confirm the analysis of the melting traces presented here.

The absence of degradation was verified by infrared analysis of the samples submitted to slow cycles of heating and cooling. However, the calorimeter is a very sensitive test of ongoing chemical reactions, which are accompanied by a heat effect. In the rare cases where unusual heat flows occurred, the sample was disregarded. Since the kinetics of evolution of the heat flow during the melting of fraction III has a similar pattern for the samples of different origins, it is very unlikely that its origin is not from the polymer. The dispersion on the enthalpy of fusion increases understandably for fraction III which melts slowly and over a large temperature interval (20–50 h and 25–30 K). It is <5 J for $H_1 + H_2$.

Results and Discussion

The results consist of endotherms of fusion (Figures 1 and 2) and of fusion and crystallization (Figures 4–6) for the GUR as received or annealed. Melting traces are also given in Figure 7 for three samples of medium and low MW. The characteristics of melting and crystallization are presented in Table I which is divided in four sections for easier reading. The results are in the following order: (A) for the nascent, (B) for the annealed, (C) for the solvent-annealed, and (D) for the low MW samples.

Figures 1 and 2 are typical melting endotherms of nascent GUR at three values of v, namely, 1 K/h for Figures 1 and 3 and 6 K/h for Figure 2. Fusion occurs in three steps corresponding to three fractions whose meltings have been separated by the slow rate of temperature increase. Fraction I is associated with low MW, fraction II with unconstrained crystals, and fraction III with constrained crystals in equilibrium with a constrained melt. Fraction III which is not clearly identifiable at $v > 1$ K/h will not be commented upon further. In Figure 3, the temperatures of the ends of fusion (T(I), T(II), and T(III)) and the enthalpies of fusion are plotted against v for the different fractions. $H_1 + H_2$ have not been separated in Figure 3, but the relevant values can be found in Table I. The end

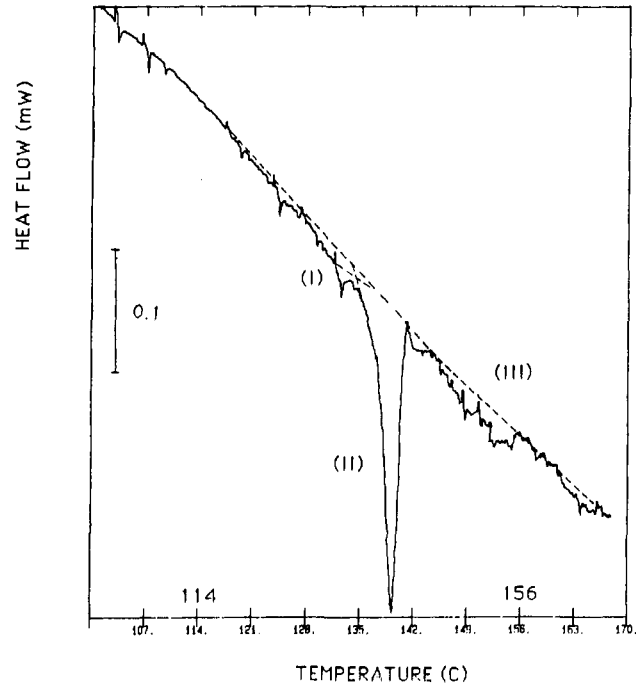

Figure 1. Melting trace of nascent GUR at v = 1 K/h showing the three fractions associated with the low MW (I), the unconstrained crystals with a peak at 139.5 °C (II), and the constrained crystals (III).

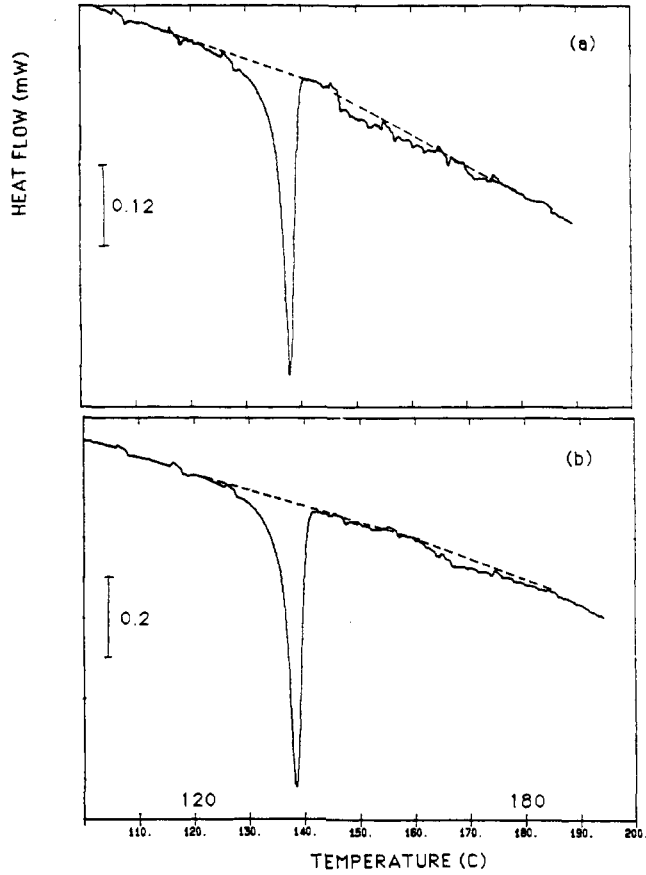

Figure 2. Melting trace of nascent GUR PE: (a) at v = 3 K/h and (b) at v = 6 K/h.

of the endotherms for fractions I and II does not depend on v for these low v, but fraction III is extremely superheatable so that at $v > 12$ K/h the endotherm is no longer visible and a quantity of crystals equivalent to about one-quarter of the total remains unmelted, giving to the melt its nonflowing characteristic[13] and birefringence.[17] In

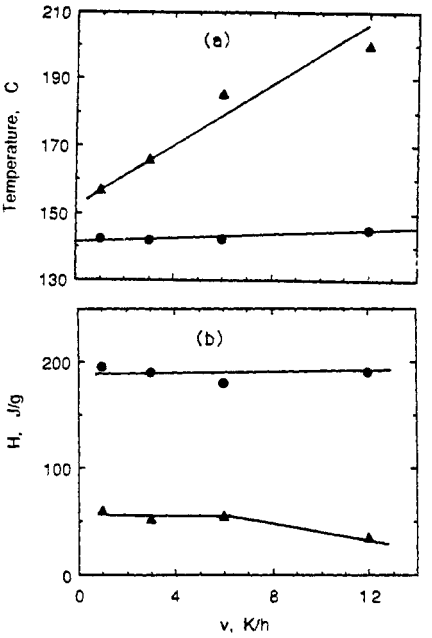

Figure 3. Characteristics of slow melting for nascent GUR: (a) temperature of the end of melting of fractions II (●) and III (▲) and (b) heats of melting of the fractions I + II (●) and III (▲) against v in Kelvin per hour.

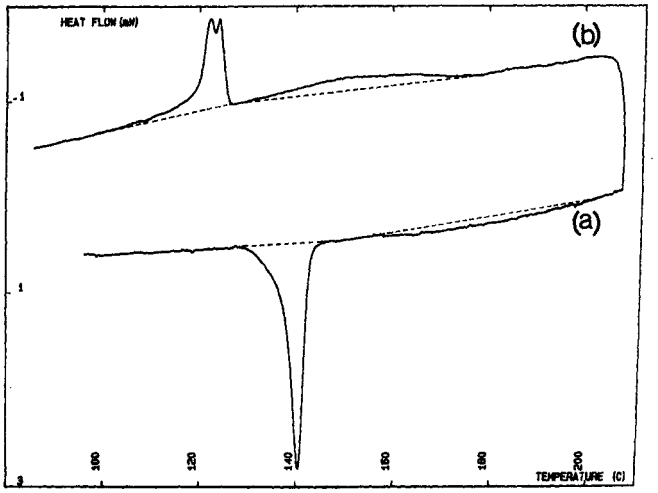

Figure 4. Melting and crystallization traces at $v = 12$ K/h of the nascent sample. The value of H_3 at the fusion (30 J/g) indicates an incomplete fusion during the time alloted (4 h) between 150 and 200 °C. Fraction III recrystallizes at 176 °C and has the expected H_3 (60 J/g); 122–124 °C is the crystallization of chain-folded crystals from disordered melt.

Figure 3b, the enthalpies of fusion, $(H_1 + H_2)$ and H_3 are seen to depend little on v when v is small. For $v = 12$ K/h, the low value of H_3 (30 J/g instead of 60 J/g) reflects an incomplete fusion. The overall observed crystallinity for $v < 12$ K/h is 0.87, comparable to that obtained by other methods in which equilibrium was ascertained. After annealing, the overall crystallinity increases to 0.90–0.95 as seen in the column before the last one of Table I. At $v > 12$ K/h, the absence of H_3 makes the calorimetrically determined crystallinity drop to 0.70. When possible, H_3 has been decomposed in two, $H_{3,a}$ and $H_{3,b}$ whose tentative identification is given below. In fusions made at $v > 1$ K/h and for annealed samples with slower kinetics of melting, $H_{3,b}$ is not detectable. The possibility of stored elastic energy released during fusion will not be commented upon here.

The melting and crystallization traces at $v = 12$ K/h of the nascent sample are given in Figure 4. The peak at

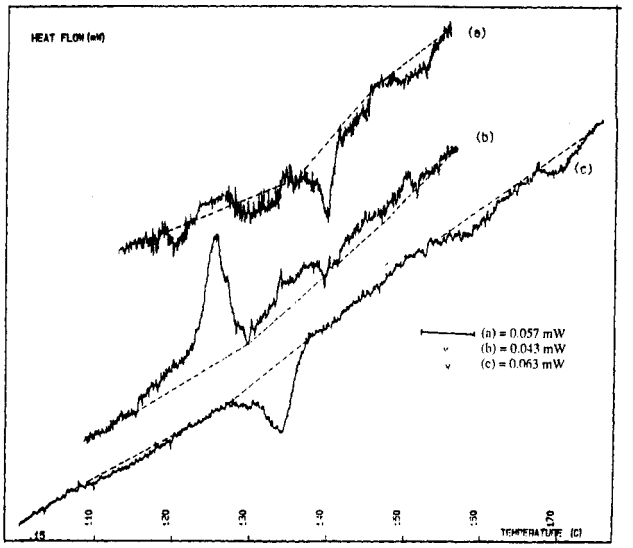

Figure 5. Extensively annealed sample. (a) Melting trace at $v = 0.5$ K/h. The three fractions of Figure 1 are seen with more details such as 122–128 °C exotherm of recrystallization and split (142–154 °C) of fraction III; $H_3 = 54$ J/g. (b) Crystallization trace at $v = 1$ K/h of the sample melted at $v = 0.5$ K/h. Fraction III recrystallizes between 155 and 129.5 °C; $H_3 = 73$ J/g. At 125 °C, the chain-folded crystals crystallize from disordered melt. (c) Melting trace at $v = 1$ K/h after the crystallization of Figure 5b. Note that H_3, now 106 J/g, is situated at higher temperature than in the first fusion (a).

122–124 °C is the expected crystallization exotherm of the orthorhombic chain-folded crystals from a disordered melt. Due to the fast crystallization of chain-folded crystals, the temperature of the peak of crystallization does not depend much on v as can be verified from the three traces of crystallization shown, i.e., at 12 in Figure 4b and 1 K/h in Figures 5b and 6b. The flat exotherm between 179 and 130 °C suggests recrystallization of fraction III as such, i.e., without loss of much strain. To confirm this result, crystallization traces have been recorded on annealed samples at lower v.

Fusion, Crystallization, and Second Fusion of Extensively Annealed Samples. Isothermal annealing or annealing with plateaus of temperature induce complex and sometimes nonequilibrium changes in the solid.[3] For maximum stabilization of the initial state of the nascent sample, it was submitted to an extensive annealing which consisted either of a slower melting at 0.5 K/h or of a week-long annealing at 120 °C followed by quenching to room temperature. Figures 5 and 6 are the traces of the first fusion, first crystallization, and second fusion of these samples whose characteristic features are listed in Table I, section B.

The positions of the maxima in heat flow for melting or crystallization of fraction II are unchanged by the treatment. The comparable values of T_f, the final temperature of melting, and H_{total} indicate a similar melting process between the annealed and nascent samples. The end of melting for fraction III (168–170 °C) may be inexact due to some uncertainty about the end of the melting trace at $v = 0.5$ K/h (Figure 5a). Fraction III recrystallizes slowly between 155 and 130 °C with two separate endotherms. Lower molecular weights crystallize slowly within a low-temperature range. The heat flow could not be detected since it is within the baseline, but their endotherms of melting are clear between 110 and 120 °C. The enthalpy for crystallization of fraction I which was not measured has been written (in parentheses in Table I) equal to the enthalpy of fusion of the same fraction.

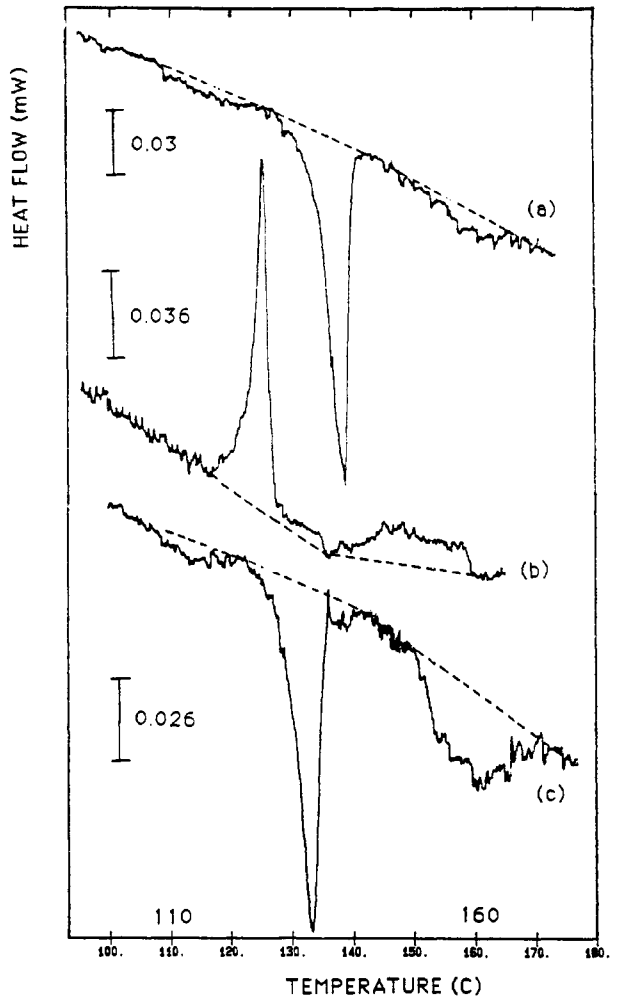

Figure 6. Extensively annealed sample (1 week at 120 °C): (a) melting trace showing the three fractions, $H_1 = 22$, $H_2 = 203$, and $H_3 = 50$ J/g; (b) crystallization trace, $H_3 = 73$ J/g, $H_2 = 160$, and H_1 occurring below 100 °C is not recorded; (c) melting trace after crystallization of Figure 5b, $H_1 = 20$, $H_2 = 134$, and $H_3 = 113$ J/g, $v = 1$ K/h.

Arrested Melting and Identification of Fraction III. Between fractions I + II and fraction III, melting is arrested during a temperature interval which depends on the thermal history and v. In the second melting (of Figures 5c and 6c), the interval (10–15 K, i.e., 10–15 h) is larger than in the first fusion because T_m (I+II) is lower in the second fusion. The arrest and resumption of the melting imply that, in the course of melting of fractions I + II, a parameter takes on some importance which it did not have at the beginning of the melting. This parameter is likely to be the strain, f, which develops in the unmelted crystals through the tie molecules in the melt. The melting temperature under strain, $T_{m,f}$, increases with strain; i.e., $T_{m,f} = T_{m,o}(1 + kf)$, $T_{m,o}$ being the melting temperature without strain. The melting resumes only when T has reached the value of $T_{m,f}$ of the system. For a crystal deformed, at constant pressure, with a constant tensile force applied in one direction $k = \Delta l/\Delta S$ where Δl is the change of length due to the retraction on melting and ΔS, the augmentation of entropy. The network in UHMWPE is unlike that in the drawn fibers, and k depends on other parameters. Knowing the complex morphology of nascent UHMWP, one can expect multidirectional tensile forces which vary across the sample and lead to a range of T_m. Since fraction III has been observed for samples of different origins and submitted to a variety of treatments, one can say that the strain is not only a vestige of polymerization

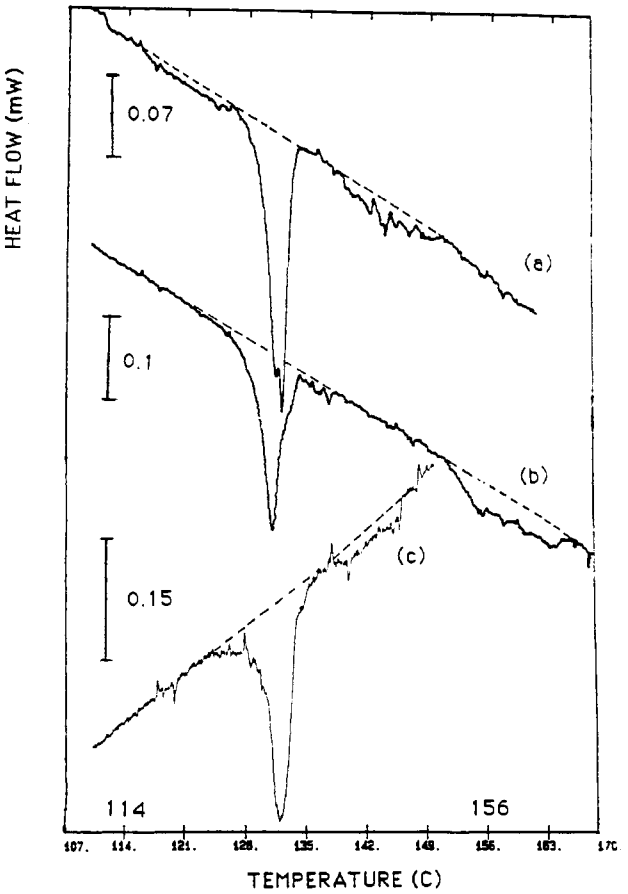

Figure 7. Melting traces for medium and low MW samples: (a) sample 1483, $M_w = 32\,100$, $M_w/M_n = 1.11$, $H_3 = 45$ J/g; (b) Marlex, $M_w = 155\,000$, $M_w/M_n = 10$, $H_3 = 81$ J/g; (c) sample 1484, $M_w = 119\,600$, $M_w/M_n = 1.19$, $H_3 = 32$ J/g.

conditions but a feature of partial melting. The formation of a network during partial melting has been recognized early on (Jenckel and Wilsing (1949) quoted in ref 3, p 135). The range of melting temperature has been attributed to a range of strain, the smaller cystals probably bearing a larger strain than the large ones. However, the change of T_m may also be due, as for a binary solid solution, to a change of composition of the phases during melting. A thermodynamical model for the melting of the complex mixture made of strained and linked crystals and strained and unstrained melt would be worthwile to develop. The presence of unmelted crystals gives a simple explanation to the two phases and the memory found in the melt. The tight knots tentatively suggested as responsible for the unexpected characteristics of the melt[20] may well exist between the crystals, but their measurement has to be indirect. The results of second melting suggest that strain can be stored as well as released during a thermal history. The values for H_3 increase after the slow crystallization to 95 (Figure 5c) and 113 J/g (Figure 6c), the higher value corresponding to the annealed sample. The reason is likely to be a perfection of the crystals without reduction of tie molecules so that more crystals melt under strain than in the first fusion. The increased perfection of the crystals should be seen in a corresponding rise of the overall enthalpy of fusion, H_{total}. However, a quantitative measurement of small differences in H_{total} may be obscured by the increased temperature stability of the perfected crystals which melt more slowly. Consequently, the values of the temperatures in the high-temperature tail of the melting endotherm should be used in combination with H_{total} to identify the strain melting of perfected crystals.

Table I
Characteristics of Melting and Crystallization of GUR ($M_w = 0.9 \times 10^6$) at Low v ($0.5 < v < 12$ K/h). Data for Low and Medium MW

sample		v, K/h	H_1, J/g	H_2, J/g	T_2, °C	$H_{3,a}$, J/g	$H_{3,b}$ J/g	H_{total}, J/g	figure
nascent (A)									
	1st melting	1	45 (119.0–137.0)[a]	150	140.7 (134.0–142.1)	60 (142.1–157.0)	20 (162.1–167.5)	275	1
	1st melting	3	<5	190	139.3 (118.0–141.8)	52 (148.0–166.2)	[b]	242[d]	2a
	1st melting	6	<5	180	139.3 (118.0–142.2)	55 (161.4–185.3)	[b]	235[d]	2b
	1st melting	12	0	190	140.5 (128.0–145.0)	35 (156.0–200.0)	[b]	225[d]	4a
	1st crystallization	12	(20)[c]	140	122.3–124.1 (100.0–127.0)	61 (130.0–179.0)		221	4b
extensively annealed (B)									
	1st melting[e]	0.5	25 (118.5–133.8)	148	140.0 (135–141.9)	43 (141.9–145.3)	54 (148.4–154.8)	270	5a
	1st crystallization	1	(26)[c]	177	125.4 (115.8–129.5)	47 (129.5–139.8)	26 (139.8–155.0)	276	5b
	2nd melting	1	26 (108.4–121.0)	168	134.3 (124.8–138.0)	65 (153.6–167.2)	30 (167.2–173.6)	289	5c
	1st melting[f]	1	22 (107.8–124.0)	203	140.3 (127.8–142.9)	51 (147.2–170.3)		276[d]	6a
	1st crystallization	1	(20)[c]	160	126.1 (117.4–136.9)	73 (136.9–161.4)		253[d]	6b
	2nd melting	1	20 (105.8–122.9)	134	134.4 (122.9–141.6)	113 (150.9–174.6)		267[d]	6c
solvent-annealed[g] (C)									
in decalin	1st melting	1	10 (126.0–135.0)	193	139.6 (133.1–142.2)	45 (141.2–153.3)	[h]	248[d]	
	1st melting	3	15 (118.4–133.0)	184	138.9 (129.0–142.3)	34 (146.5–171.5)	[h]	233[d]	
in TCB	1st melting	1	20 (125.2–135.5)	210	139.5 (132.5–142.2)	10 (141.2–147.3)	[h]	240[d]	
	1st melting	3	25 (117.1–135.0)	196	139.7 (132.0–144.5)	10 (144.0–161.0)	[h]	231[d]	
low and medium MW (D)									
1483	1st melting	1	30 (116.5–127.2)	200	132.5–134.1 (127.2–135.5)	45 (139.0–152.0)		275	7a
Marlex	1st melting	1	0	211	132.5 (122.0–140.0)	81 (152.3–166.5)		292	7b
1484	1st melting	1	30 (123.8–129.4)	232	132.0 (127.6–135.6)	32 (138.4–145.7)		294	7c

[a] Temperature interval of melting. [b] $H_{3,b}$ is not visible for $v > 1$ K/h. [c] The value of H in parentheses means that the corresponding endotherm below 100 °C has not been recorded. [d] When $H_{3,b}$ is missing, H_{total} is low and T_f is higher than that reported in the column of $H_{3,a}$. [e] Nascent GUR at $v = 0.5$ K/h. [f] Annealed in a sealed tube under N_2 atmosphere, 120 °C during 1 week. [g] Annealed in a sealed tube under N_2 atmosphere, 90 °C during 1 week in the presence of a solvent. [h] T_{max} was too low to observe $H_{3,b}$.

For the second fusion, the range of melting temperature of fraction III is the same or higher than that of the first fusion. It is noteworthy that by contrast the overall original strain in the nascent which leads to a T_m of the main peak equal to 140 °C is never recovered in the successive crystallizations since the T_m of the main peak in the successive fusions is situated 5–6 K lower than the T_m of the nascent polymer. The high-temperature exotherms observed in Figures 4–6 are a sure indication that the high-temperature endotherms do not correspond to the enthalpy of disordering of the melt. A disordered melt recrystallizes at 130 °C, not at 160–170 °C. Furthermore, the size of H_3 is too high to correspond only to an enthalpy of disordering.

Annealing in a Solvent below T_d. Annealing was also achieved in solvents about 10 K below the dissolution temperature, T_d, of fractions I + II. The results are given in Table I, section C, for decalin and trichlorobenzene (TCB) as an illustration of the selective effect of some solvents on crystal reorganization below T_d. In decalin, the amount of fraction III ($H_{3,a} = 45$ J/g at $v = 1$ K/h) is similar to that of the nascent while in TCB it has been reduced by a factor of about 4 ($H_{3,a} = 10$ J/g). In these runs, the temperature has not been raised high enough to see the $H_{3,b}$ endotherm so that H_{total} is too small. However, the sum of $H_1 + H_2$ is a good indication of what H_3 will be. In the early stages of the present work on gels, it was the large differences in $H_1 + H_2$ when solvent or thermal history were modified which led to the search for fraction III. Although it is satisfactory to melt completely the sample and obtain the balance of the total melting enthalpy (280–290 J/g) between the fractions, strain melting can be identified otherwise. The specific effect of thermal history or solvent treatment can be observed from quantitative analysis of fractions I + II only, in cases where the heat of fusion of fraction III is not available. The T_m of fraction II (139.6 °C) has remained high since melting has not occurred during the annealing. Commentaries on the origin of this solvent effect are reported elsewhere, with other comparative results in the two solvents.[20] The interesting point of these results is that the different metastable states created in the crystals by their immersion either in decalin or in TCB have remained different during solvent evaporation and the lengthy annealing associated with the melting at $v = 1$ K/h.

A manifestation of strain melting is a two-step melting, the pseudohexagonal phase being an intermediate between the orthorhombic crystals and the melt. Among the traces of fraction III presented here, some show clearly a two-step melting (Figures 1 and 5c) or two-step crystallization (Figure 5b); others do not. A range of strain in the network is likely to be the origin of the overlapping and smearing of the endotherms corresponding to the two steps.

The present results and in particular Figure 3 showing the dependence on v of the temperature of fusion of fraction III have made clear the importance of time for melting fraction III or observing the pseudohexagonal phase in nascent UHMWPE. Failure to see it by Raman spectroscopy[22] for instance is probably due to the fact that, in these experiments, a long time at high temperature was incompatible with adequate measurements.

Comparison of Constrained Melting in Nascent and Processed UHMWPE. The large increase of T_m of fraction III can be discussed by comparison with other conditions where T_m is raised. In the homogeneous system constituted by the melt crystallizing as extended chains under pressure, melting temperatures equivalent to those of fraction III (and of the pseudohexagonal phase) are reached with external pressures between 1 and 2 kbars. The kinetics of melting at atmospheric pressure of pressure-crystallized PE is slow[3] and similar to that of nascent. Constrained extended fibers on the other hand, can be made to have an equilibrium melting over a few minutes below 160 °C.[20] Furthermore, fibers melted under strain are known to be damaged by the process and are not likely to recrystallize at high temperature as does the

melt of UHMWPE. Clearly, the melting of nascent UHMWPE cannot be compared quantitatively with the melting of fibers. Our understanding of this phenomenon is based on the necessary solution step for the formation of a film, the stock material for fibers. The preparation of a solution from the nascent which includes vigorous stirring distributes the strained melt evenly in the solvent. Cooling establishes a network first in the solution and later among the crystals after solvent evaporation. This process by forming material more homogeneous than the nascent permits the drawing of the film but also makes fraction III less stable in temperature in the film than it was in the nascent polymer. The T_m of fraction III are explained qualitatively by regions of constraint in the partially melted nascent as high or higher than in the melt of constrained fibers.

Slow Melting of Medium and Low MW Samples. In Figure 7 and in Table I, section D, the results of slow melting of low and medium MW are given at $v = 1$ K/h. The three fractions are seen as in the GUR with a H_3 which is large (81 J/g) for the highest MW (Marlex, $M_w = 155\,000$, $M_w/M_n = 10$) and medium for the samples with a lower MW (32–45 J/g). Further work is in progress on these samples to investigate the stability on cooling of fraction III.[23] None of these samples are nascent, but their last processing (extrusion or fractionation from solution) goes back to a few years, leaving open the possibility of reorganization with time. The existence of fraction III in medium and low molecular weight samples leads us to question the origin of strain melting, associated in the previous comments with long chains and perfect crystals. Polydispersity of the samples seems to be as important as high molecular weight since samples Marlex and 1484 with similar M_w but different values of M_w/M_n show different amounts of fraction III. Since the end groups of the methylene chains are known to enter the crystalline lattice, one can speculate that large and thick perfect crystals can grow from shorter chains and melt with strain.

Conclusion

The slow fusion reveals that, during fusion, high MWPE behaves like a two-phase system, the strain-free crystals (fractions I + II) and the strained crystals (fraction III). This new fraction is likely to be a network whose crystalline junctions are unmelted crystals stabilized in temperature due to strain. Eventually, after an arrest in melting, the network melts (possibly never completely). The trace of melting obtained with the C80 calorimeter gives a quantitative confirmation to suggestions of never-melted crystals found in the literature. In the time/temperature scheme of the experiment, about 30 h in the temperature cycle (typically 10 h from 170 to 180 °C and 20 h from 180 to 160 °C), the melted network is not randomized and recrystallizes as a network at high temperature. The amount of network in the polymer (about 25%) depends on several parameters such as thermal history, M_w, and MWD (molecular weight distribution) whose specific roles are not well identified. Slow crystallization leads to an increase of fraction III due to crystal perfection. Unmelted crystals give a simple explanation for the long-term memory and heterogeneity in the melt and for the too low crystallinity found by calorimetry. The implications of these results are important for polymer characterization, preparation and study of dry gels, mechanical properties of films, and compatibility of UHMWPE with other PE's and for the origin of thermoreversible gels as discussed in the following paper in this issue. It is hoped that investigations by other techniques might further the understanding of the high-temperature endotherms of PE either by confirming the explanations presented here or by providing other ones.

Acknowledgment. The support of the Natural Sciences and Engineering Research Council of Canada is gratefully acknowledged.

References and Notes

(1) Phuong-Nguyen, H.; Delmas, G. *Macromolecules*, following paper in this issue.
(2) Pennings, A. J.; Zwijnenburg, A. *J. Polym. Sci., Polym. Phys. Ed.* **1979**, *17*, 1011.
(3) Wunderlich, B. *Macromolecular Physics*; Academic Press: New York, 1976; Vol. 2; 1980; Vol. 3.
(4) Kresteva, M.; Nedkov, E.; Radilova, A. *Colloid Polym. Sci.* **1985**, *263*, 273.
(5) Chanzy, H. D.; Bonjour, E.; Marchessault, R. H. *Colloid Polym. Sci.* **1974**, *252*, 8.
(6) Keller, A.; Willmouth, F. M. *Makromol. Chem.* **1969**, *121*, 42.
(7) Furuhata, K.; Yokokawa, T.; Seoul, Ch.; Miyasaka, K. *J. Polym. Sci., Polym. Phys. Ed.* **1986**, *24*, 59.
(8) Cohen-Addad, J. P.; Feio, G.; Péguy, A. *Polym. Commun.* **1987**, *28*, 255.
(9) Folland, R.; Charlesby, A. *Eur. Polym. J.* **1979**, *19*, 953.
(10) Nedkov, E.; Kresteva, M. *Bulg. J. Phys.* **1982**, *9*, 63.
(11) Kresteva, M.; Nedkov, E.; Sinigerska, E.; Krestev, V. J. *Macromol. Sci. Phys.* **1982**, *B21* (3), 383.
(12) Basset, D. C.; Block, S.; Piermarini, G. J. *J. Appl. Phys.* **1974**, *45*, 4146.
(13) Clough, S. B. *J. Macromol. Sci. Phys.* **1970**, *B4*, 199.
(14) Smook, J.; Pennings, A. J. *Colloid Polym. Sci.* **1984**, *262*, 712.
(15) Murthy, N. S.; Correale, S. T.; Kavesh, S. *Polym. Commun.* **1990**, *31*, 50.
(16) Wunderlich, B.; Czornyj, G. *Macromolecules* **1977**, *10*, 906.
(17) Gopalan, M.; Mandelkern, L. *J. Polym. Sci., Polym. Phys. Ed.* **1970**, *8*, 8223.
(18) Czornyj, G.; Wunderlich, B. *Makromol. Chem.* **1977**, *178*, 843.
(19) Rijke, A. M.; Mandelkern, L. *J. Polym. Sci., Polym. Phys. Ed.* **1967**, *5*, 71, 3833.
(20) Phuong-Nguyen, H. Ph.D. Thesis, McGill University, Montreal, Canada, 1991.
(21) de Gennes, P.-G. *Macromolecules* **1984**, *17*, 703.
(22) Wunder, S. *J. Polym. Sci., Polym. Phys. Ed.* **1986**, *24*, 99.
(23) Phuong-Nguyen, H.; Delmas, G. Unpublished work.

Registry No. Hostalen GUR 413, 9002-88-4.